Analysis of Three-Phase Rectifiers with Constant-Voltage Loads

Vahe Caliskan David J. Perreault Thomas M. Jahns[†] John G. Kassakian

Laboratory for Electromagnetic and Electronic Systems
Massachusetts Institute of Technology
Cambridge, Massachusetts 02139

[†]Department of Electrical and Computer Engineering
University of Wisconsin
Madison, Wisconsin 53706

Abstract— **This paper presents a quantitative analysis of the operating characteristics of three-phase bridge rectifiers with ac-side reactance and constant-voltage loads. We describe the operating characteristics of the three-phase diode bridge rectifier in continuous conduction mode. Simple approximate expressions are derived for the output current characteristic, as well as the input power factor. The output current control characteristic is also derived for the three-phase thyristor bridge converter with constant-voltage load. The derived analytical expressions are applied to a practical example and simulations are utilized to validate the analytical results.**

I. Introduction

In a number of power electronics applications, one encounters a three-phase bridge rectifier supplied from an inductive ac source driving a constant-voltage load, as illustrated in Figure 1. For example, this often occurs in battery charger/power supply systems, such as employed in automotive and aerospace applications. The three-phase source with series inductance represents the alternator back emf and armature inductance, while the constant-voltage load represents the battery and system loads. A similar situation occurs when a transformer-driven rectifier is loaded with a capacitive (rather than inductive) output filter. Here, the ac-side inductance is due to line and transformer leakage reactances, while the dc-side filter acts as a constant-voltage load. In all such applications, the rectifier input and output currents are functions of the system voltage levels and the ac-side reactance, and are also functions of firing angle if thyristor devices are used (Figure 2).

While one might expect that analytical models for the operational characteristics of the systems of Figures 1 and 2 would be readily available in the literature, this appears not to be the case. The behavior of single-phase diode rectifier circuits with ac-side impedance and capacitive loading have been treated in the work of Schade and others [1]–[6]. Most treatments of three-phase rectifier circuits only consider operation with inductive (constant-current) loading of the rectifier. Schaefer [7] does devote a chapter to rectifiers with ac-side reactance and capacitive loading, with a primary focus on single-phase circuits and the three-phase midpoint connection circuit. The three-phase bridge rectifier is treated for the light-load (discontinuous conduction mode) case, but the chapter stops short of fully analyzing the bridge rectifier in continuous conduction, noting that the analysis is complex. The literature seems to be even more sparse regarding operating characteristics of thyristor bridges with constant-voltage loads, though the principles involved are sometimes described [7] and the challenging nature of firing angle control in this case is occasionally mentioned [7], [8].

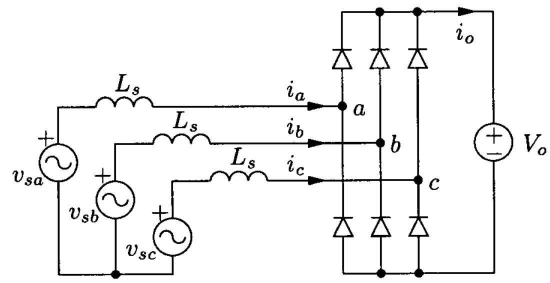

Figure 1: Three-phase diode bridge rectifier.

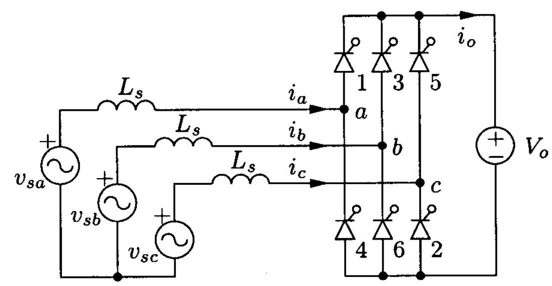

Figure 2: Phase-controlled three-phase bridge rectifier.

This paper presents a quantitative analysis of the operating characteristics of bridge rectifiers with ac-side reactance and constant-voltage loads. Section II describes the operating characteristics of the three-phase diode bridge

0-7803-5421-4/99/$10.00

rectifier in continuous conduction mode. Simple approximate expressions are derived for the output current characteristic (output current as a function of input reactance and input and output voltages), as well as the input power factor and distortion. In Section III, the output current control characteristic is derived for the three-phase thyristor bridge converter with constant-voltage load. Section IV of the paper applies these newly-derived analytical expressions to a practical example, and validates the results against simulations.

II. Three-Phase Diode Rectifier with Constant-Voltage Load

A three phase rectifier with a voltage source load is shown in Figure 1. Also included are line inductances L_s each in series with sinusoidal voltages v_{sa}, v_{sb} and v_{sc} which are a three phase set of voltages with magnitude V_s and angular frequency ω. The diodes in the full bridge rectifier are assumed ideal except for a finite on-voltage, V_d. Assuming that the source currents i_a, i_b and i_c are continuous, it can be shown that the line-line voltages v_{ab}, v_{bc} and v_{ca} are given by

$$v_{ab} = \frac{V_o'}{2}\left[\mathrm{sgn}(i_a) - \mathrm{sgn}(i_b)\right] \tag{1}$$

$$v_{bc} = \frac{V_o'}{2}\left[\mathrm{sgn}(i_b) - \mathrm{sgn}(i_c)\right] \tag{2}$$

$$v_{ca} = \frac{V_o'}{2}\left[\mathrm{sgn}(i_c) - \mathrm{sgn}(i_a)\right] \tag{3}$$

where sgn(•) is the signum function and $V_o' = V_o + 2V_d$. Based on the above line-line voltages, the combination of the full bridge rectifier and voltage source load can be replaced by three line-neutral voltage sinks given by

$$v_a' = V_o''\,\mathrm{sgn}(i_a) \tag{4}$$

$$v_b' = V_o''\,\mathrm{sgn}(i_b) \tag{5}$$

$$v_c' = V_o''\,\mathrm{sgn}(i_c) \tag{6}$$

where $V_o'' = V_o'/2 = V_o/2 + V_d$. Let us further approximate the voltage sinks v_a', v_b' and v_c' by their fundamental components, v_{a1}', v_{b1}' and v_{c1}', respectively, since the fundamental component is the only one contributing to power transfer. This approximation yields

$$v_a' \approx v_{a1}' = \frac{4V_o''}{\pi}\sin(\omega t - \phi) \tag{7}$$

$$v_b' \approx v_{b1}' = \frac{4V_o''}{\pi}\sin(\omega t - \phi - 2\pi/3) \tag{8}$$

$$v_c' \approx v_{c1}' = \frac{4V_o''}{\pi}\sin(\omega t - \phi + 2\pi/3) \tag{9}$$

where ϕ is the phase angle between each voltage source and and its corresponding voltage sink for each phase. Given

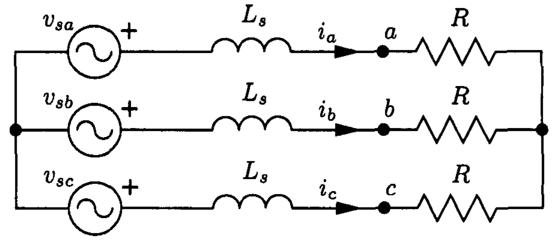

Figure 3: Simplified model of the three-phase diode rectifier.

expressions (7)–(9), we can also approximate the inductor currents i_a, i_b and i_c by their fundamental components i_{a1}, i_{b1} and i_{c1}, respectively. Furthermore, since we know voltages v_{a1}', v_{b1}' and v_{c1}' are in phase with their respective line currents, the inductor currents will have the form

$$i_a \approx i_{a1} = I_{s1}\sin(\omega t - \phi) \tag{10}$$

$$i_b \approx i_{b1} = I_{s1}\sin(\omega t - \phi - 2\pi/3) \tag{11}$$

$$i_c \approx i_{c1} = I_{s1}\sin(\omega t - \phi + 2\pi/3) \tag{12}$$

where I_{s1} is the magnitude of the fundamental component of the line currents yet to be determined. Now, the voltage sources v_{a1}', v_{b1}' and v_{c1}' may be replaced by equivalent resistors R_{ab}, R_{bc} and R_{ca}, respectively, given by

$$R_{ab} = R_{bc} = R_{ca} = \frac{4V_o''}{\pi I_{s1}} \triangleq R \tag{13}$$

The equivalent circuit for our simplified three phase full bridge rectifier is shown in Figure 3.

To determine the magnitude of the fundamental component of the line current, we only need to examine one of the phases. For example, the phasor line current in phase a is given by

$$\mathbf{I}_a \triangleq I_{s1}e^{-j\phi} = \frac{V_s}{\sqrt{R^2 + (\omega L_s)^2}}e^{-j\tan^{-1}(\omega L_s/R)} \tag{14}$$

Substituting the expression for I_{s1} into (13), equivalent resistance R may now be written as

$$R \triangleq \frac{4V_o''}{\pi I_{s1}} = \frac{4V_o''\sqrt{R^2 + (\omega L_s)^2}}{\pi V_s} \tag{15}$$

Solving for R in (15) yields

$$R = \frac{(4V_o''/\pi)\,\omega L_s}{\sqrt{V_s{}^2 - (4V_o''/\pi)^2}} \tag{16}$$

Note that our approximation for the equivalent resistance is valid if and only if $\pi V_s/4V_o'' > 1$. Using the expression for the equivalent resistance R in (16), the magnitude of the fundamental of the line current I_{s1} and the phase angle ϕ can be expressed as

$$I_{s1} = \frac{\sqrt{{V_s}^2 - (4V_o''/\pi)^2}}{\omega L_s} \tag{17}$$

$$\phi = \tan^{-1}\sqrt{(\pi V_s/4V_o'')^2 - 1} \tag{18}$$

The average output current delivered to the voltage source load V_o can be approximated as

$$\langle i_o \rangle \approx \frac{3}{\pi} I_{s1} = \frac{3}{\pi}\frac{\sqrt{{V_s}^2 - (\frac{4V_o''}{\pi})^2}}{\omega L_s} \tag{19}$$

The power factor k_p may now be computed using the expression for ϕ

$$k_p \approx \cos\phi = \frac{4V_o''}{\pi V_s} \tag{20}$$

The expressions for the average output current and power factor in (19) and (20) will be compared with results of computer simulations in Section IV. The procedure we have used in this section to analyze the three-phase diode rectifier can be applied to the single phase rectifier as well. We will not discuss the single-phase rectifier here; however, we provide some details of the analysis in the Appendix.

In our derivation of the equivalent resistance R given in (16), we included the impact of the line inductances but neglected series resistances to simplify the analysis. The inclusion of series resistance into the analysis is straightforward; however, it does complicate the expressions. For example, if we assume that each phase has a line inductance L_s and series resistance R_s associated with it, the expression for the equivalent resistance R becomes

$$R = \frac{\left(\frac{4V_o''}{\pi}\right)^2 R_s + \left(\frac{4V_o''}{\pi}\right)\sqrt{(\omega L_s)^2\left[V_s^2 - \left(\frac{4V_o''}{\pi}\right)^2\right] + R_s^2 V_s^2}}{{V_s}^2 - (4V_o''/\pi)^2} \tag{21}$$

Using (21), one can derive new expressions for I_{s1}, ϕ and k_p which include the impact of the series resistance R_s.

III. Phase-Controlled Three-Phase Rectifier with Constant-Voltage Load

A simplified schematic of a phase-controlled three phase rectifier with voltage sink is shown in Figure 2. The analysis of this system is much more difficult due to presence of thyristors and the introduction of firing angle α as an additional (control) variable. (For purposes of this paper, we define α as the electrical firing angle delay relative to the forward voltage that appears across the thyristor.) To simplify the analysis, we will assume that the on-voltage of the thyristors is zero. In order to compute the average output current, we only need to consider one of the phase currents (for example, phase b) over a half of its period of conduction. Over a half period of conduction, the current i_b contributes to the average output current over two thyristor conduction intervals: when thyristors 2 and 3 are on (conduction angle length α) and when thyristors 1, 2 and 3 are on (conduction angle length $\frac{\pi}{3} - \alpha$). Integrating i_b over each of these intervals yields:

$$Q_{2,3} \triangleq \int_0^{\alpha} i_b(\omega t)d(\omega t) = \left(i_{x1} - \frac{\sqrt{3}V_s}{2\omega L_s}\sin\theta\right)\alpha + \frac{\sqrt{3}V_s}{2\omega L_s}(\cos\theta - \cos(\theta+\alpha)) - \frac{V_o}{4\omega L_s}\alpha^2 \tag{22}$$

$$Q_{1,2,3} \triangleq \int_{\alpha}^{\frac{\pi}{3}} i_b(\omega t)d(\omega t) = \left[i_{x4} - \frac{V_s}{\omega L_s}\cos\left(\alpha + \theta - \frac{2\pi}{3}\right)\right] \cdot \left(\frac{\pi}{3} - \alpha\right) + \frac{V_s}{\omega L_s}\sin\left(\theta - \frac{\pi}{6}\right) - \frac{V_s}{\omega L_s}\sin\left(\alpha + \theta - \frac{2\pi}{3}\right) - \frac{V_o}{6\omega L_s}\left(\frac{\pi}{3} - \alpha\right)^2 \tag{23}$$

where i_{x1}, i_{x4} and θ are defined as follows

$$i_{x1} = \frac{V_s}{\omega L_s}\left(\cos(\theta+\alpha) - \cos\left(\theta + \frac{\pi}{3}\right)\right) - \frac{V_o}{3\omega L_s}\left(\frac{\pi}{3} - \alpha\right) \tag{24}$$

$$i_{x4} = i_{x1} + \frac{\sqrt{3}V_s}{2\omega L_s}(\sin(\theta+\alpha) - \sin\theta) - \frac{V_o\alpha}{2\omega L_s} \tag{25}$$

$$\theta = \cos^{-1}\left(\frac{V_o(\frac{4\pi}{3} - \alpha)}{-12V_s\sin(\frac{\alpha}{2} - \frac{\pi}{6}) + 6\sqrt{3}V_s\sin(\frac{\alpha}{2})}\right) - \frac{\alpha}{2} \tag{26}$$

The average output current due to i_b over a full conduction period is

$$\langle i_o \rangle\Big|_{i_b} = \frac{1}{2\pi}\left(2\left[Q_{1,2} + Q_{1,2,3}\right]\right) \tag{27}$$

Therefore, the average output current for the entire thyristor bridge is

$$\langle i_o \rangle = 3\langle i_o \rangle\Big|_{i_b} = \frac{3}{\pi}\left[Q_{1,2} + Q_{1,2,3}\right] \tag{28}$$

The expressions for the average output current (28) will be compared with results of computer simulations in Section IV.

IV. Example Applications

The models that were discussed in the last two sections form the basis of a number of machines. For example, the system shown in Figure 1 is an often used model of an automotive alternator which is based on a special type of synchronous machine called the claw-pole (Lundell) generator.

In this section, we present some numerical examples that verify the validity of the simplified models that were developed in the last two sections. We will compare our analytical results with ones obtained from a circuit simulator.

First, consider the full bridge rectifier given in Figure 1 with the following parameter values: $V_o = 14.5$ V, $L_s = 180$ μH, $V_d = 1$ V. The results of our comparison are shown in Figures 4–6. Figure 4 shows the average output current $\langle i_o \rangle$ versus the magnitude of the source voltage V_s with the source frequency f ($\omega = 2\pi f$) fixed at 180 Hz. Figure 5 shows the average output current $\langle i_o \rangle$ versus the source frequency f with the source voltage V_s fixed at 20 V. Figure 6 depicts the power factor k_p versus the source voltage V_s with the source frequency f fixed at 180 Hz. In Figures 4 and 5, analytical results are obtained by the use of (19) and while the symbol ($\times$) represents the results from circuit simulation. In Figure 6, (20) was used to generate the analytical results. As can be seen from these comparisons, there is good agreement between the simulated and analytical results.

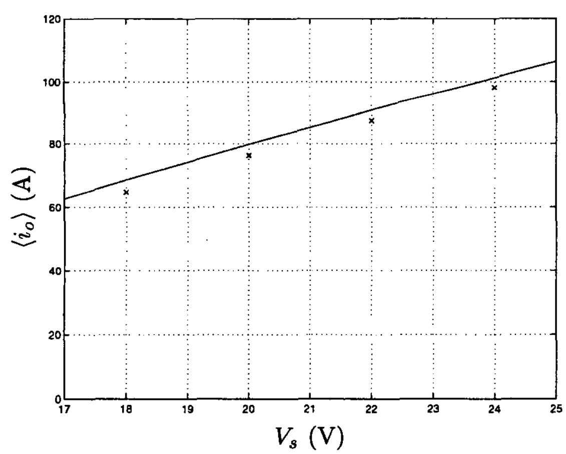

Figure 4: Average output current $\langle i_o \rangle$ versus source voltage magnitude V_s with $f = 180$ Hz (solid: analytical, $\times$: simulation).

Second, consider the phase-controlled rectifier shown in Figure 2 with the following parameter values: $V_s = 24$ V, $f = 180$ Hz, $V_o = 14.5$ V, $L_s = 180$ μH. The results of our analysis is shown in Figure 7. The plot shows the

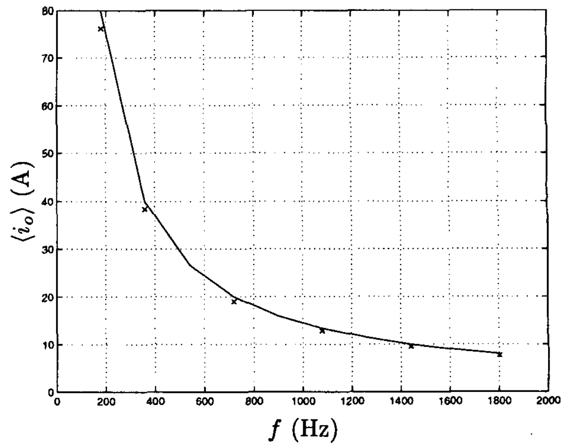

Figure 5: Average output current $\langle i_o \rangle$ versus frequency f with $V_s = 20$ V (solid: analytical, $\times$: simulation).

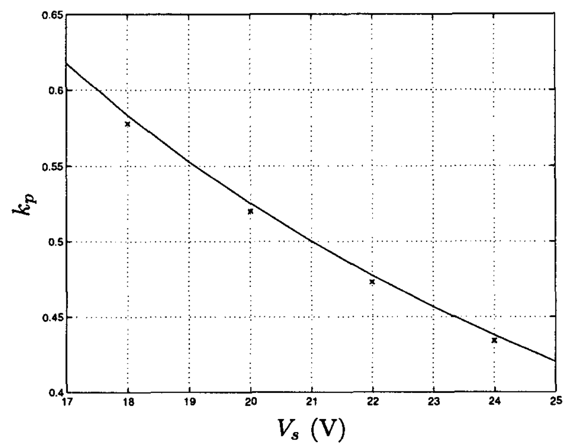

Figure 6: Power factor k_p versus source voltage magnitude V_s with $f = 180$ Hz (solid: analytical, $\times$: simulation).

average output current $\langle i_o \rangle$ versus the firing angle α of the thyristors. The solid line obtained by the use of (28) while the symbol ($\times$) represents the results from circuit simulation. Once again, there is good agreement between the analytical and simulation results.

V. Conclusion

In this paper, we have presented an analysis of bridge rectifier characteristics with ac-side reactance and constant-voltage loads operating in continuous conduction mode. Approximate expressions were derived for the output current characteristics and power factor of three-phase diode bridge rectifiers. The inclusion of series resistance of phases was also described. We also derived the approximations for the output current characteristics of thyristor bridge rectifiers. The approximate analytical expressions

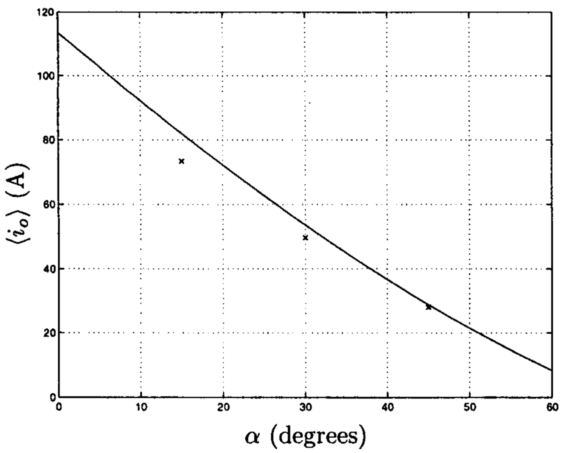

Figure 7: Average output current $\langle i_o \rangle$ versus firing angle α for $V_s = 24$ V, $f = 180$ Hz, $V_o = 14.5$ V, $L_s = 180$ μH (solid: analytical, $\times$: simulation).

for both types of bridge rectifiers were compared to computer simulations and were shown to be quite accurate.

Appendix

Single-Phase Diode Rectifier with Constant-Voltage Load

A single-phase rectifier with a voltage source load is illustrated in Figure 8. Sinusoidal voltage source v_s ($=V_s \sin(\omega t)$) with the a series line inductance L_s drives the bridge. As in the three-phase rectifier, the diodes in the bridge rectifier are assumed ideal except for a finite on-voltage, V_d.

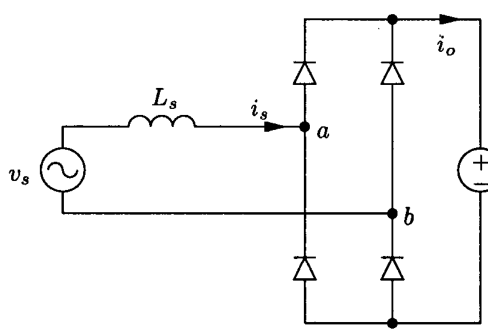

Figure 8: Single-phase diode bridge rectifier.

Assuming that the source current i_s is continuous, voltage v_{ab} can be expressed as

$$v_{ab} = V_o' \,\mathrm{sgn}(i_s) \tag{29}$$

where sgn($\bullet$) is the signum function and $V_o' = V_o + 2V_d$. We can approximate the voltage v_{ab} by its fundamental component, $v_{ab,1}$ since the fundamental component is the only one contributing to power transfer:

$$v_{ab} \approx v_{ab,1} = \frac{4V_o'}{\pi} \sin(\omega t - \phi) \tag{30}$$

where ϕ is the phase angle between v_{ab} and i_s. The line current i_s can also be approximated by its fundamental component i_{s1}.

$$i_s \approx i_{s1} = I_{s1} \sin(\omega t - \phi) \tag{31}$$

where I_{s1} is the magnitude of the fundamental component of the line current. As in the three-phase rectifier, the voltage sources $v_{ab,1}$ may be replaced by an equivalent resistor R_{ab} given by

$$R_{ab} = \frac{4V_o''}{\pi I_{s1}} \tag{32}$$

The equivalent circuit for our simplified single-phase full bridge rectifier is shown in Figure 9.

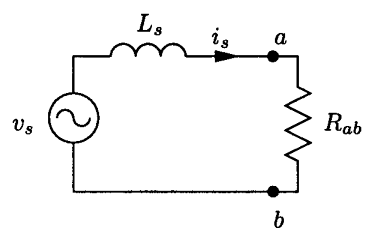

Figure 9: Simplified model of the single-phase diode rectifier.

To determine an expression for the equivalent resistance, we first compute the phasor line current

$$\mathbf{I}_s \triangleq I_{s1} e^{-j\phi} = \frac{V_s}{\sqrt{R^2 + (\omega L_s)^2}} e^{-j \tan^{-1}(\omega L_s / R)} \tag{33}$$

The equivalent resistance R_{ab} may now be written as

$$R_{ab} \triangleq \frac{4V_o'}{\pi I_{s1}} = \frac{4V_o' \sqrt{R_{ab}^2 + (\omega L_s)^2}}{\pi V_s} \tag{34}$$

Solving for R_{ab} in the above equation gives

$$R_{ab} = \frac{(4V_o'/\pi)\,\omega L_s}{\sqrt{{V_s}^2 - (4V_o'/\pi)^2}} \tag{35}$$

Using the above expression for the equivalent resistance R_{ab}, the magnitude of the fundamental of the line current

I_{s1} and the phase angle ϕ can be expressed as

$$I_{s1} = \frac{\sqrt{{V_s}^2 - (4V_o'/\pi)^2}}{\omega L_s} \tag{36}$$

$$\phi = \tan^{-1}\sqrt{(\pi V_s/4V_o')^2 - 1} \tag{37}$$

The expressions for R_{ab}, I_{s1} and ϕ are very similar to the three-phase rectifier in which the voltage term V_o' is replaced by V_o''. The expression for the average output current is

$$\langle i_o \rangle \approx \frac{2}{\pi} I_{s1} \tag{38}$$

ACKNOWLEDGMENT

The authors would like to acknowledge the support for this research provided by the member companies of the MIT/Industry Consortium on Advanced Electrical/Electronic Components and Systems.

REFERENCES

[1] O.H. Schade, "Analysis of rectifier operation," *Proceedings of IRE*, vol. 31, no. 7, pp. 341–361, July 1943.

[2] P. Richman, "Wave factors for rectifiers with capacitor input filters, and other high crest factor loads," *IEEE Transactions on Industrial Electronics and Control Instrumentation*, vol. 21, no. 4, pp. 235–241, November 1974.

[3] A.G. Bogle, "Rectifier circuit performance: some new approximate formulas," *Proceedings of IEE*, vol. 124, no. 12, pp. 1127–1134, December 1977.

[4] A. Lieders, "Single-phase rectifier circuits with CR filters, part 1 – theory," *Electronic Components and Applications*, vol. 1, no. 3, pp. 153–163, May 1979.

[5] W.P. Gibbons, "Current and voltage waveform distortion analysis on three-phase "wye" power systems with rectifier loads," *IEEE Transactions on Industry Applications*, vol. 19, no. 2, pp. 181–190, March/April 1983.

[6] K.S. Hall, "Calculation of rectifier-circuit performance," *Proceedings of IEE - Part A*, vol. 127, no. 1, pp. 54–60, January 1980.

[7] J. Schaefer, *Rectifier Circuits: Theory and Design*, Wiley, 1965.

[8] G. Seguir, *Power Electronic Converters: AC-DC Conversion*, North Oxford Academic, 1986.